Electronic Supplementary Information

The β- and γ-NiFeOOH electrocatalysts for efficient oxygen evolution reaction: an aspect from the electrochemical activation energy

Zheng Lin, Pengpeng Bu, Ye Xiao, Qiulu Gao and *Peng Diao**

School of Materials Science and Engineering, Beihang University, Beijing 100191, P. R. China

*Corresponding Author Email: pdiao@buaa.edu.cn.

Supplementary Details of Experimental Section

Chemical Reagents

Nickel foam (NF, 99.9%, 110 PPI, 1.7 mm thickness) was purchased from Shanxi Lizhiyuan Battery Materials Co., Ltd. Nickel (II) sulfate hexahydrate ($NiSO_4 \cdot 6H_2O$, 99%), iron (II) sulfate heptahydrate ($FeSO_4 \cdot 7H_2O$, 99.95%) and potassium hydroxide (KOH, 99.99%) were purchased from Shanghai Macklin Biochemical Co. Ltd. Boric acid (H_3BO_3, 99.5%), hydrochloric acid (HCl, 36%~38%), ethanol (C_2H_5OH, 99.7%) and acetone (CH_3COCH_3, 99.5%) were purchased from Beijing Chemical Reagents Co., Ltd. All the chemical reagents were used as obtained without further purification. Aqueous solutions were prepared with deionized water (18 MΩ·cm).

Characterization

The crystal structures of the catalysts were analyzed by X-ray powder diffractometry on a Rigaku D/Max 2500 (Rigaku Industrial Co., Ltd.) equipped with a filtered Cu-Kα radiation. All the catalysts characterized by XRD are scratched off from corresponding electrodes and collected as powders. The morphology and elemental distribution of the catalysts was characterized by JSM-7500 (JEOL Co., Ltd.) field emission scanning electron microscopy (FESEM). Transmission electron microscopy (TEM) images, high-resolution TEM (HRTEM) images and STEM-EDS elemental mapping images were acquired on a JEM-2100F (JEOL Co., Ltd.) field emission microscope with an accelerating voltage of 200 kV. X-ray photoelectron spectroscopy (XPS) measurements were conducted on a Thermo Scientific K-Alpha (Thermo Fisher Sci. Co., Ltd.) equipped with an Al-Kα source (1486.6eV) operating at a vacuum pressure of 10^{-7} mbar. All binding energies were calibrated to the C1s orbit at 284.8 eV. Raman spectra were acquired on a HORIBA LabRAM HR Evolution instrument (HORIBA Sci. Co., Ltd.) with a 633-nm laser source.
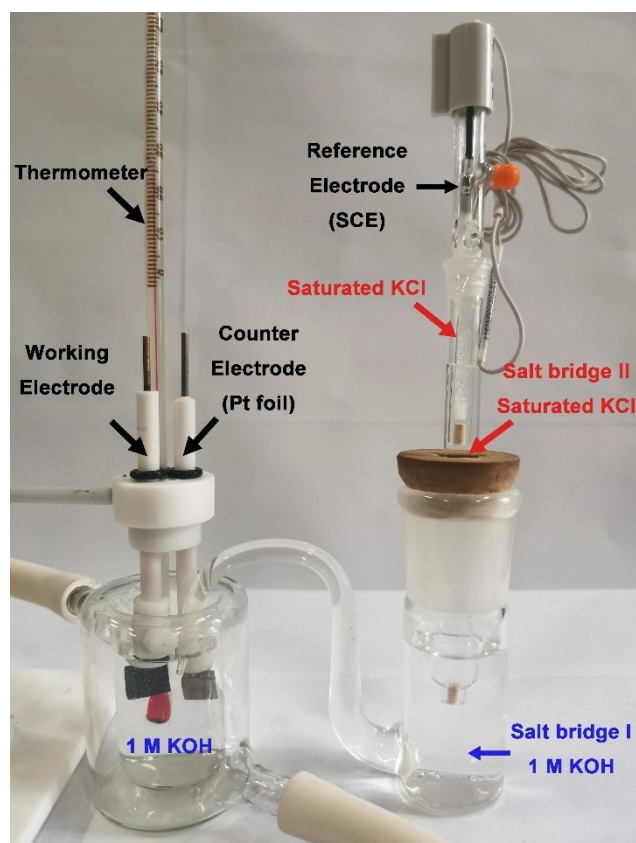
Fig. S1 The cell setup for temperature tests to measure the electrochemical activation energy. The working and counter electrodes were placed in a jacketed electrochemical cell and the temperature was controlled by circulating water from an external thermostatic water bath. The reference electrode was placed in the salt bridge vessel which was connected to the electrochemical cell by a Luggin-Haber capillary. The reference electrode was kept at room temperature during the test.
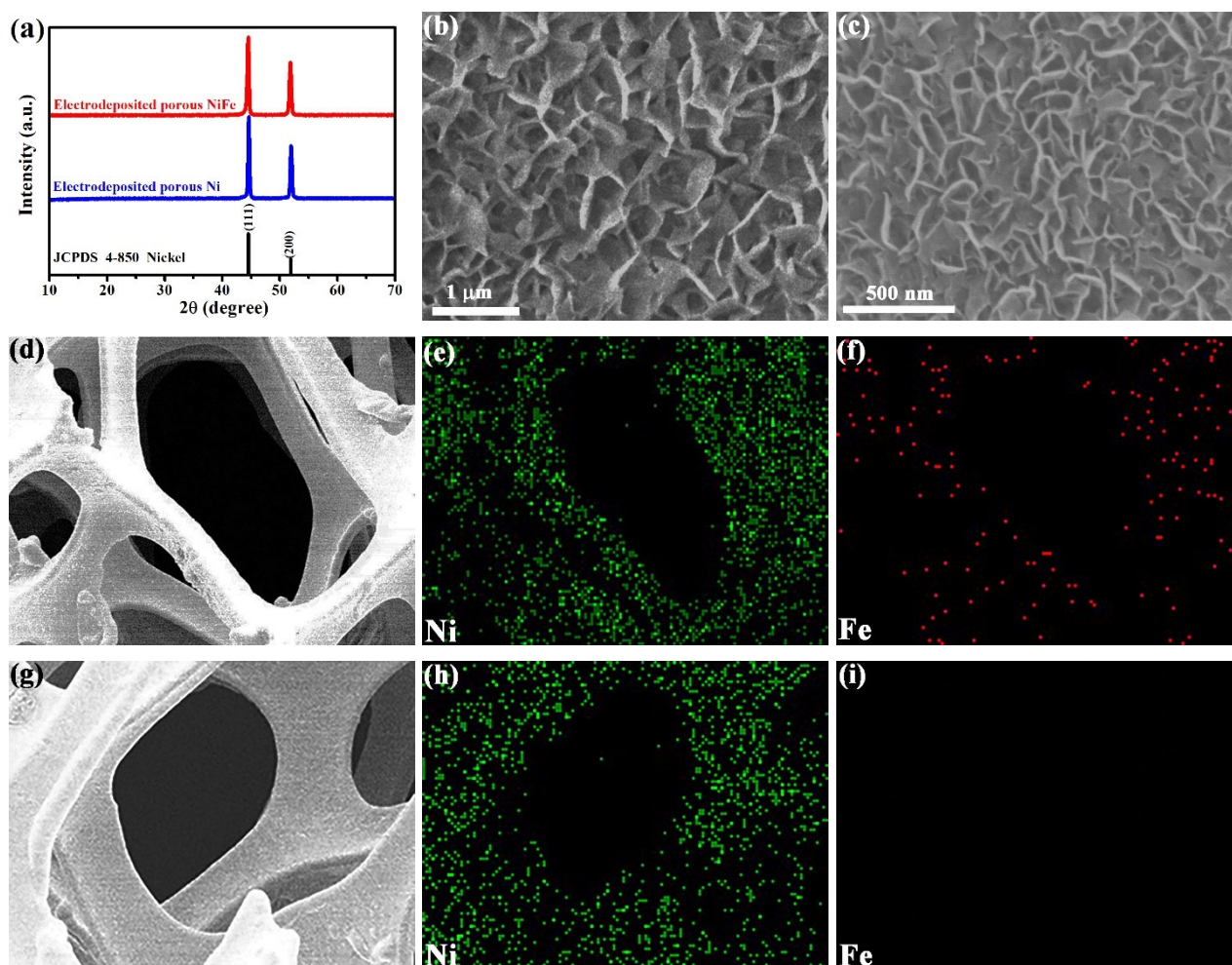
Fig. S2 (a) The XRD patterns of NiFe and Ni nanosheets electrodeposited on NF. The identical XRD patterns of NiFe and Ni indicate that the doping of small amount of Fe into Ni nanosheets does not change their crystal structure. The typical SEM images of (b) NiFe/NF and (c) Ni/NF, showing the porous network structure composed of the intersected NiFe and Ni nanosheets, respectively. The morphology and EDS elemental mapping images of NiFe/NF (d-f) and Ni/NF (g-i).
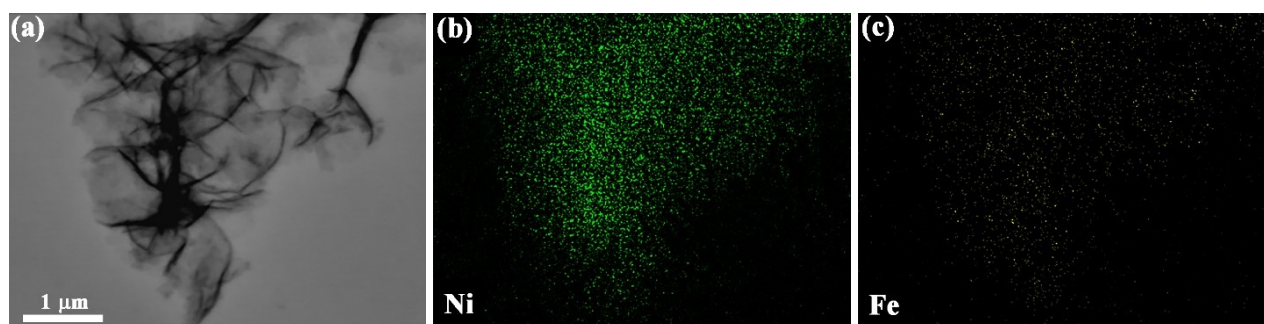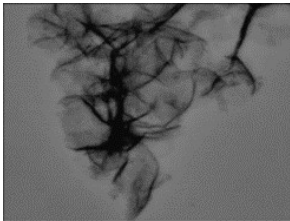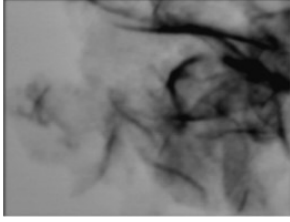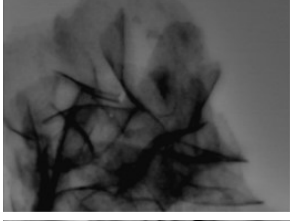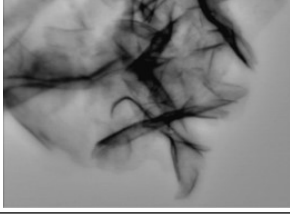

Fig. S3 STEM-EDS mapping analysis of the β-NiFeOOH, with (a), (b), and (c) showing the morphology, Ni and Fe signals of the selected region, respectively.

Table S1 Ni: Fe atomic ratio for β-NiFeOOH derived from STEM-EDS mapping analysis

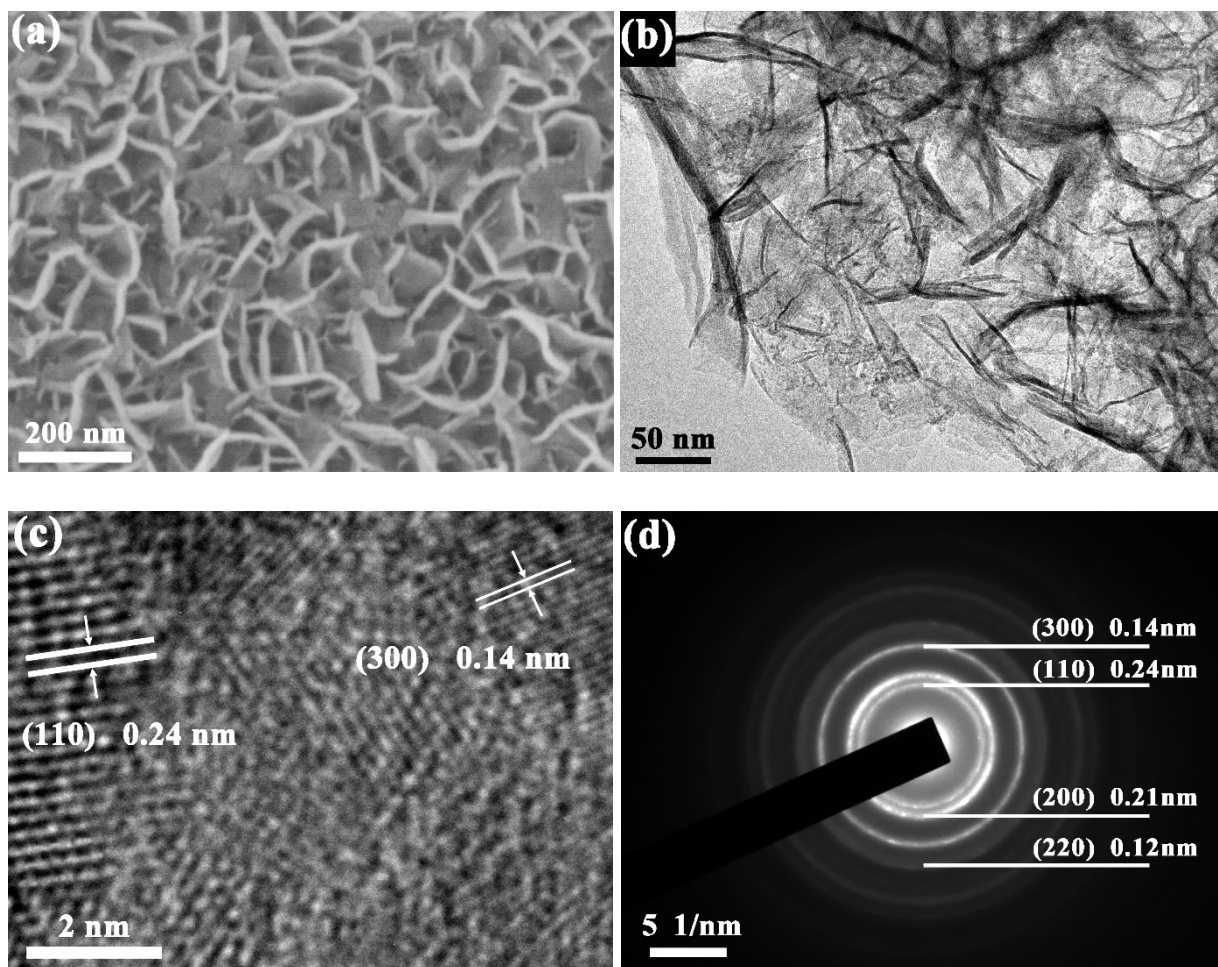| Region	Morphology	Ni: Fe atomic ratio	Average Ni: Fe atomic ratio
1		13.9: 1	
2		15.0: 1	
3		15.6: 1	14.9: 1
4		15.2: 1	

Fig. S4 (a) SEM, (b) TEM, (c) high-resolution TEM images and (d) SAED pattern of the γ-NiFeOOH prepared by electrooxidation in 1.0 M KOH. The lattice fringes and diffraction pattern are indexed to the planes of JCPDS 27-764.
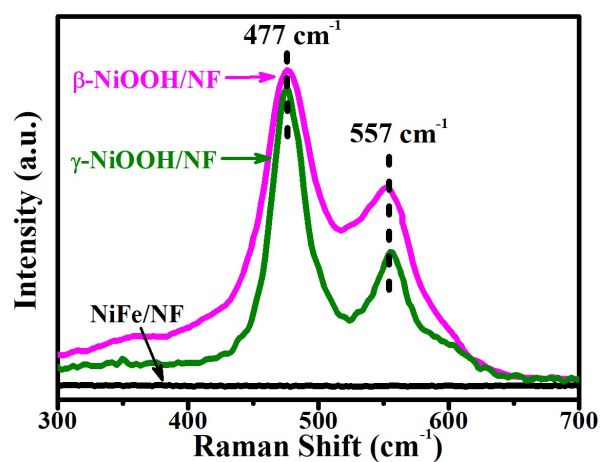

Fig. S5 Raman spectra of the β-NiOOH/NF prepared by ozonation in deionized water, the γ-NiOOH/NF prepared by electrooxidation, and bare NF.
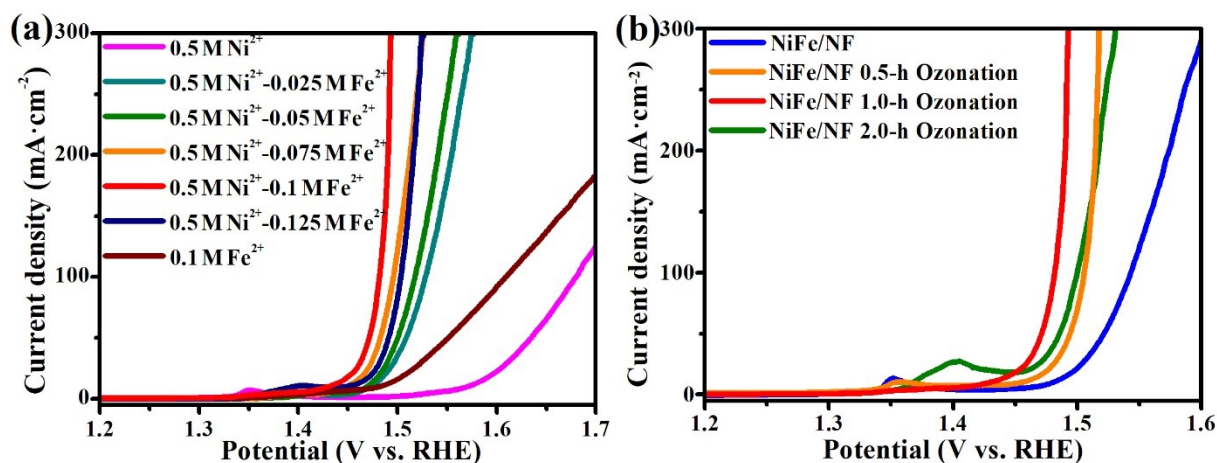
Fig. S6 The influence of preparation conditions of β-NiFeOOH/NF on its activity for the OER. (a) The LSV curves obtained on different β-NiFeOOH/NF samples synthesized by 1-h ozonation of the NiFe/NF precursors, which were prepared via electrodeposition in the 0.5 M H_3BO_3 solutions containing different concentrations of $NiSO_4$ and $FeSO_4$. (b) The influence of ozonation time on the activity of the obtained β-NiFeOOH/NF catalyst. The NiFe/NF samples electrodeposited in the mixed solution of 0.5 M H_3BO_3, 0.5 M $NiSO_4$ and 0.1 M $FeSO_4$ were used in (b) as the bimetallic precursors for ozonation. **The optimized sample for the OER were synthesized by 1-h ozonation of the NiFe/NF electrodeposited in the mixed solution of 0.5 M H_3BO_3, 0.5 M $NiSO_4$ and 0.1 M $FeSO_4$.**

Table S2 Linear fitting equations of $E_a \sim \eta$ relations for different catalysts.

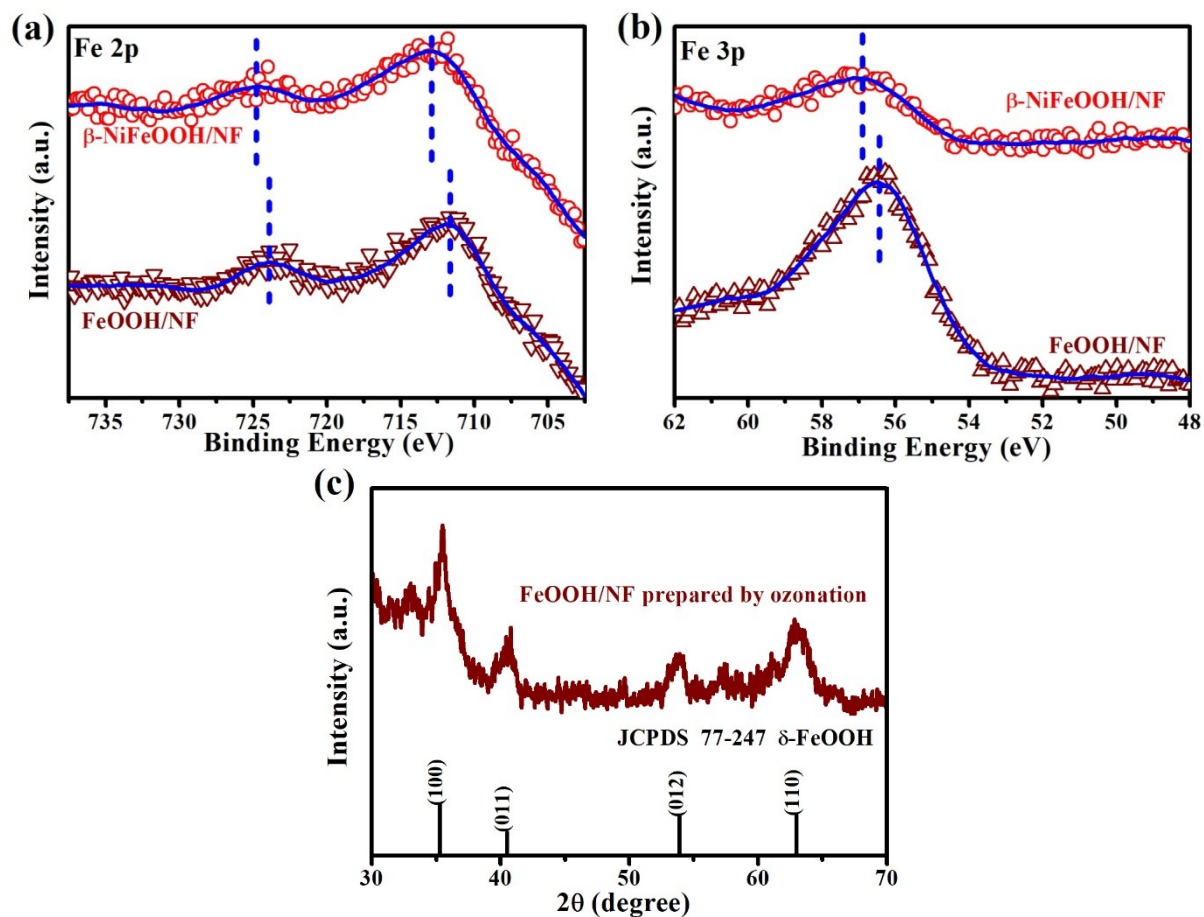| Catalyst	$E_a \sim \eta$ Linear Fitting Equation	$E_a{}^{\eta=0}$ (kJ·mol^{-1})	$\eta_{(E_a=0)}$ (mV)
β-NiFeOOH	$E_a = 89.1 - 0.254 \cdot \eta$	89	350
γ-NiFeOOH	$E_a = 101.3 - 0.268 \cdot \eta$	101	375
β-NiOOH	$E_a = 122.8 - 0.228 \cdot \eta$	123	538

Fig. S7 Comparison of the high-resolution XPS spectra of β-NiFeOOH/NF and FeOOH/NF in (a) Fe 2p and (b) Fe 3p regions. (c) The XRD pattern of the FeOOH/NF, which confirms the successful preparation of FeOOH/NF via the same ozonation procedure as that of β-NiFeOOH/NF using the Fe/NF as the metallic precursor.
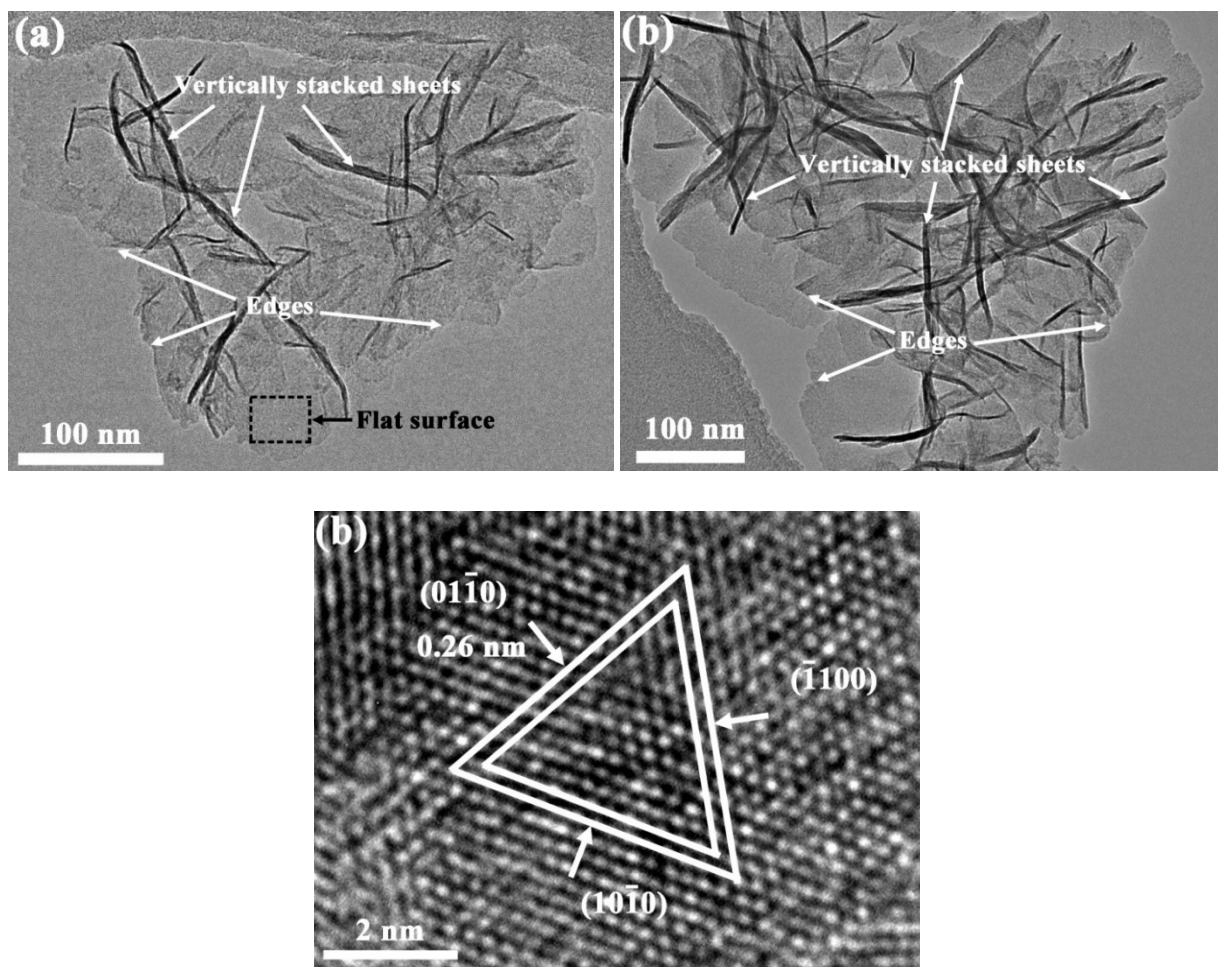
Fig. S8 (a,b) TEM images of the edges and vertically stacked nanosheets of β-NiFeOOH. (c) high-resolution lattice fringes of the square area marked with dashed lines in (a).
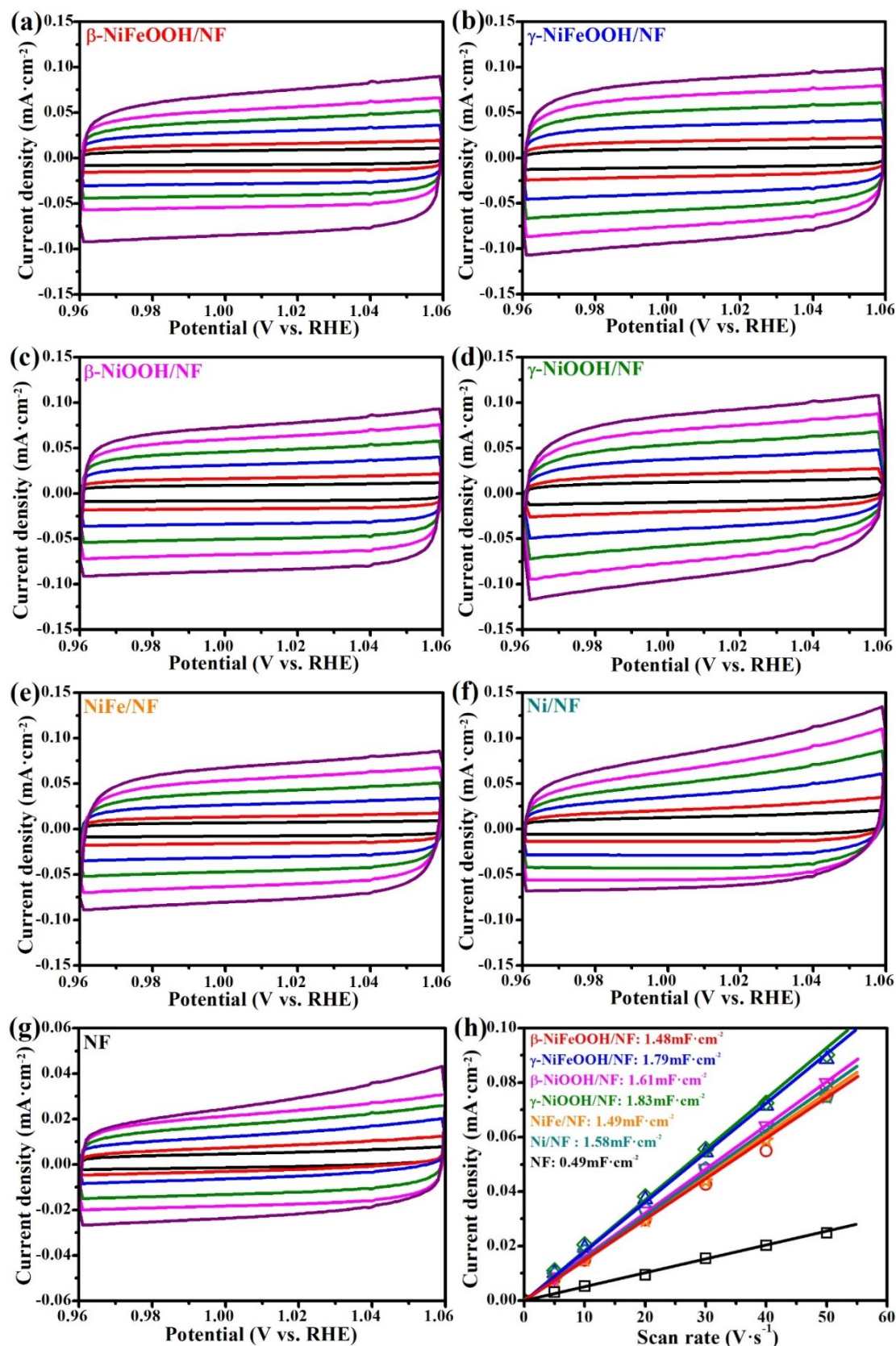
Fig. S9 CV curves recorded in 1.0 M KOH at different potential sweep rates on (a) β-NiFeOOH/NF, (b) γ-NiFeOOH/NF, (c) β-NiOOH/NF, (d) γ-NiOOH/NF, (e) NiFe/NF, (f) Ni/NF, and (g) NF. The potential sweep rates were 5, 10, 20, 30, 40, and 50mV·s⁻¹. (h) The variation of capacitive current density as a function of potential sweep rate. The slope of each fitted line represents the double-layer capacitance of the corresponding electrodes.
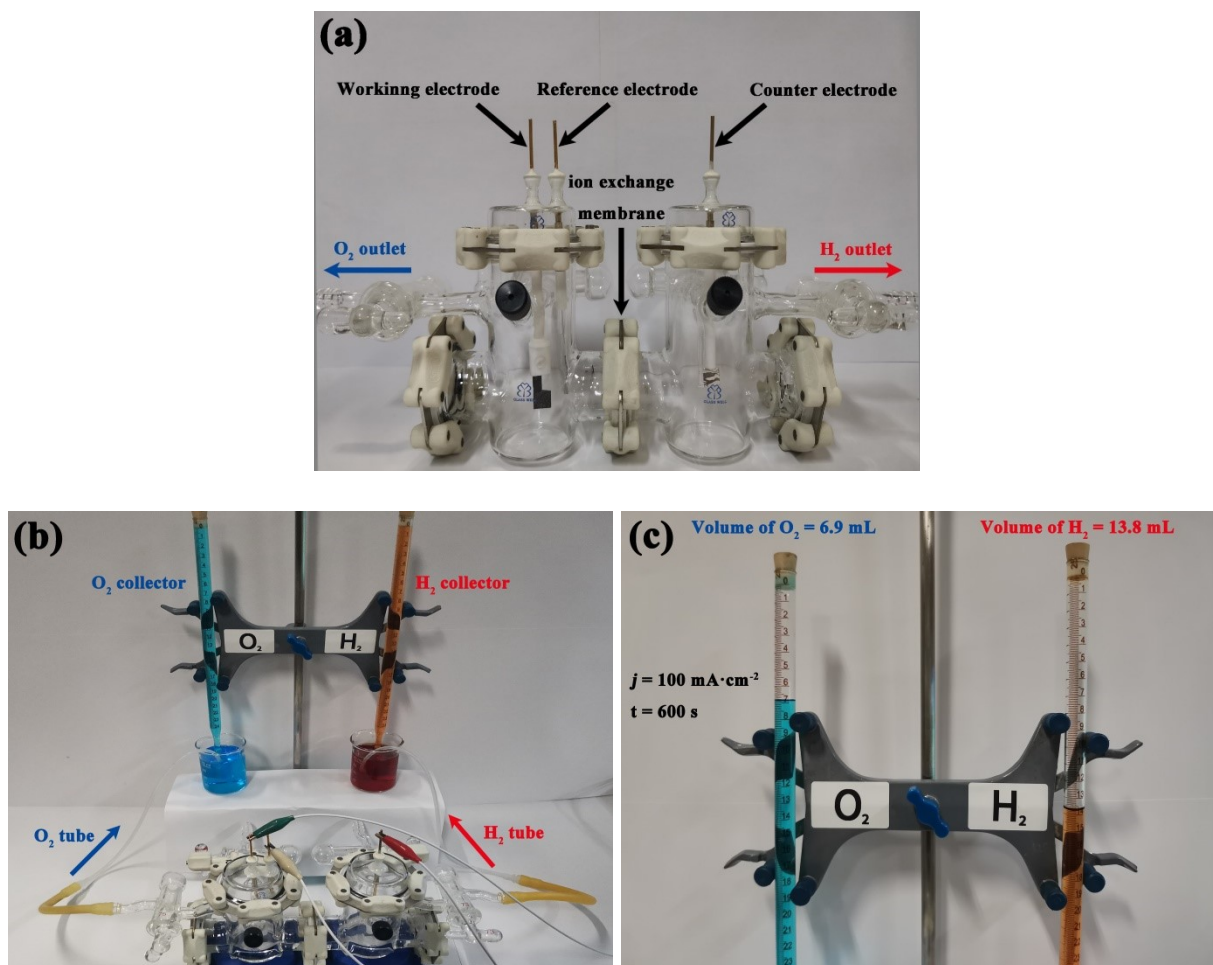
Fig. S10 (a) Digital photograph of the gas-tight two-compartment electrochemical cell. The two compartment was separated by an ion exchange membrane, and the working and reference electrodes are in one compartment while the counter electrode is in the other. (b) Digital photograph of the setup for collecting O_2 and H_2. (c) Digital photograph of O_2 and H_2 collected during the electrolysis of water at constant current of 100 mA for 600 seconds on the β-NiFeOOH/NF electrode with the geometric area of 1 cm² exposed to solution.